DALTON
FULL PAPER

Crystal supramolecularity: hexagonal arrays of sextuple phenyl embraces amongst chemically diverse compounds

Marcia Scudder and Ian Dance *

School of Chemistry, University of New South Wales, Sydney, NSW 2052, Australia

The sextuple phenyl embrace (SPE) occurs widely between molecules with XR_3 (R = aryl) moieties, and has at least quasi-three-fold symmetry. The SPE can have exact $\bar{3}$ symmetry, and therefore can be aligned with the principal axis of trigonal crystal lattices. Using the Cambridge Structural Database we report that this does occur in the crystals of a chemically diverse set of compounds, ranging from $P(C_6H_4Me\text{-}4)_3$ and Ph_3CCO_2H, through salts such as $[Ph_3PH^+]_2[Ga_2Cl_6]^{2-}$ and $[Ph_3PMe^+]_2[Cu_4I_6]^{2-}$, small molecules such as Ph_3PAlMe_3 and $Ph_3POs(CO)_3PPh_3$, to larger molecules such as $Ph_3SiOTiN(CH_2CH_2O)_3$ and $Ph_3PCu(\mu\text{-}SPh)_3U(\mu\text{-}SPh)_3\text{-}CuPPh_3(thf)_6$ (thf = tetrahydrofuran). The XR_3 moieties and the SPEs occur in hexagonal nets, and this generic crystal structure type (in space groups $R\bar{3}$, $P\bar{3}$, $R\bar{3}c$, $P\bar{3}c1$) is named the hexagonal array of sextuple phenyl embraces, HASPE. The hexagonal nets can be planar, or puckered by expansion or compression along the trigonal axis. The linkages around these hexagonal nets can be further multiple phenyl embraces, or may be elongated substantially. The non-embracing sections of the molecules can occupy the centres of the hexagons. The HASPE lattice type shows considerable flexibility in order to accommodate diverse components, but the integrity of the SPEs is maintained, attesting to their strong contribution to the lattice energy. Lower symmetry portions of molecular structure, and lower symmetry supramolecular motifs such as the $CO_2H\cdots HO_2C$ dimer, are forced to disorder by the dominant hexagonal array of SPEs. Quasi HASPE lattices with lower crystal symmetry have been recognised.

In previous papers [1–4] we have identified and described multiple phenyl embraces, which are concerted supramolecular motifs maintained by phenyl–phenyl attractive interactions. These multiple phenyl embraces are frequently dominant factors in crystal packing, and are recognisable by investigation through the Cambridge Structural Database (CSD).[5]

The dominant multiple phenyl embrace (MPE) is the sextuple phenyl embrace (SPE), structure **I**, which occurs frequently in crystals of compounds with terminal Ph_3P ligands, and in crystals containing the Ph_4P^+ cation. In the supramolecular domain of the SPE, three phenyl rings on one molecule are arrayed between three phenyl rings on the other molecule, such that each ring has edge-to-face (**ef**) interactions with two rings of the other molecule. Each phenyl ring projects two H atoms towards C atoms of a ring across the domain, and the coulombic attraction of $H^{\delta+}\cdots C^{\delta-}$ provides the directionality and some of the attractive energy of the embrace. The SPE comprises six such **ef** interactions in a cyclic sequence, as shown by the arrows in structure **I**. This SPE can have $\bar{3}$ symmetry.[4]

Another multiple phenyl embrace engaged by Ph_3P and Ph_4P^+ groups is the quadruple phenyl embrace (QPE) involving two phenyl groups on each partner, with two geometrical subclasses depending on whether the $C_{ipso}PC_{ipso}$ planes on each molecule are approximately parallel (the PQPE) or orthogonal (the OQPE).[3] The PQPE comprises one offset-face-to-face (**off**) interaction between a pair of phenyl rings, and two vertex-to-face (**vf**) interactions, while the OQPE has four **ef** interactions. The double phenyl embrace (DPE) involves an **off** interaction between one phenyl group on each molecule.

We recently reported[4] that the crystal structure of $[MePh_3P]_2[CdBr_4]$ contains pairs of $MePh_3P^+$ cations in sextuple phenyl embrace, and that these SPE are further organised in puckered hexagonal layers such that the trigonal lattice is effectively a pseudo-diamondoid array of SPE. The anions are contained in cavities surrounded by twelve cations. We named this lattice type the hexagonal array of sextuple phenyl embraces (HASPE)

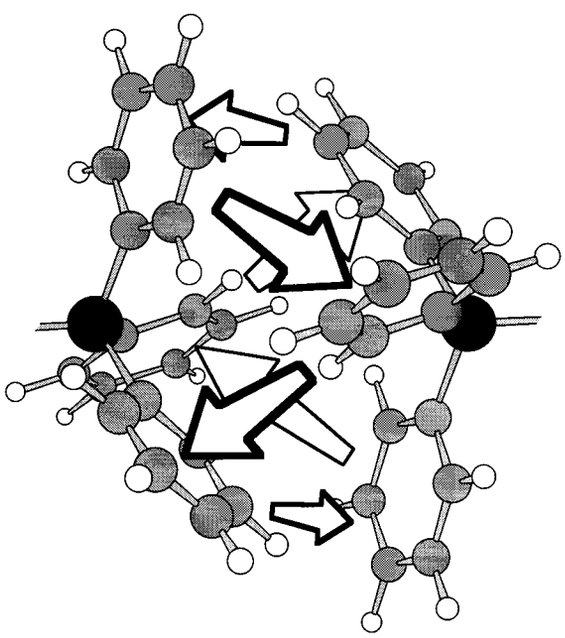

I

and noted that it could vary its dimensions in order to accommodate other anions $[CdI_4]^{2-}$ and $[Cu_4I_6]^{2-}$, and also accommodate solvent CH_2Cl_2 with $[CdBr_4]^{2-}$.

The three-fold symmetry of $MePh_3P^+$ cations allows the HASPE lattice to have exact three-fold symmetry (which can enforce disorder of the associated anion or solvent[4]). We wondered whether other molecules containing XPh_3 (or indeed XR_3, R = aryl) moieties and with potential three-fold symmetry could also crystallise with the HASPE lattice, and accordingly we interrogated the Cambridge Structural Database. We find that the HASPE lattice is prevalent amongst a variety of chemical identities and molecular structures. The HASPE lattice structure can contain other supramolecular interactions in

* E-Mail: I.Dance@unsw.edu.au

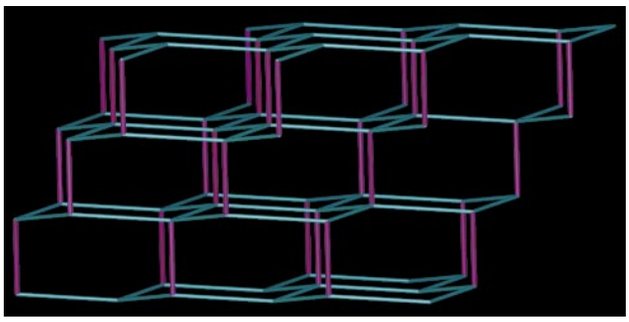

Fig. 1 The array of X atoms in a typical HASPE lattice. Each of the pink vertical rods represents an SPE, and the blue rods show the hexagonal lattice of X atoms. Every X atom is involved in one SPE

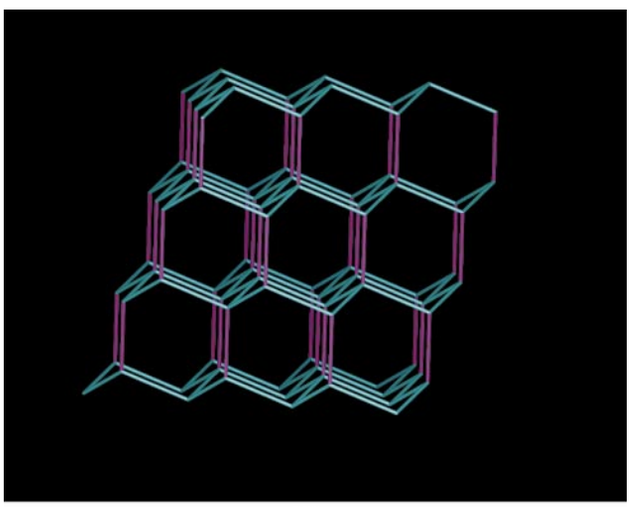

(*a*)

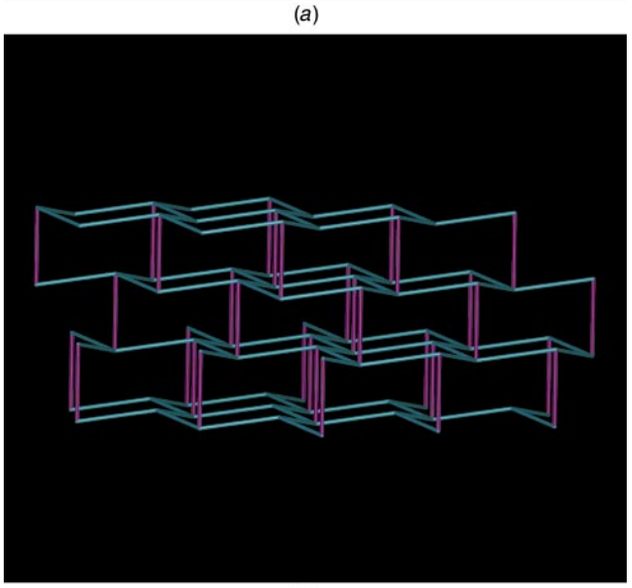

(*b*)

Fig. 2 Hexagonal lattices of SPEs (pink vertical rods) which are expanded (*a*) or compressed (*b*) along the trigonal axis, causing puckering of the hexagonal network of X atoms

addition to the SPEs, and occurs with neutral molecules as well as with cation–anion combinations. Further, the HASPE lattice can be accommodated in a variety of trigonal space groups, with a range of lattice dimensions.† It is evident that the HASPE lattice is a significant motif in crystal supramolecularity, and in this paper we describe and analyse the instances we have discovered. We are concerned also with exceptions to the HASPE lattice, for their revelations about its potency.

† This variability precludes recognition of crystal supramolecular motifs when crystallographic isomorphism alone is considered.

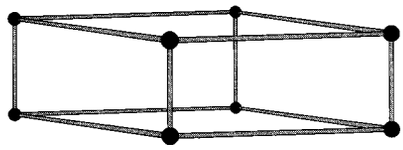

(*a*)

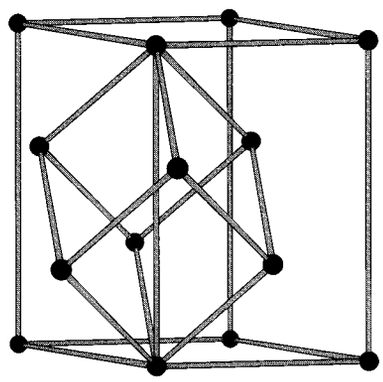

(*b*)

Fig. 3 Unit-cell relationships for HASPE lattices. (*a*) The primitive cell of space group $P\bar{3}$. (*b*) The rhombohedral cell and the hexagonal cell of space group $R\bar{3}$: the hexagonal setting contains three times as many lattice points as the rhombohedral setting

Generic Description of the HASPE Lattice

We first outline the principal characteristics of the HASPE lattice of XR_3 moieties. The predominant feature is the alignment of all SPE with the trigonal axis of a hexagonal or rhombohedral crystal lattice. Fig. 1 demonstrates the hexagonal array of X atoms in a typical HASPE and the SPEs which link them. Each X atom is involved in only one SPE, and as a consequence repetition along the hexagonal axis can occur only at the fourth layer, and stacking of the layers is . . . ABCABC . . . and cannot be . . . ABAB . . .

The hexagonal layers of X atoms need not be planar as in Fig. 1, but can be puckered by elongation or compression along the hexagonal axis, as illustrated in Fig. 2. This variability of placement of the SPEs along the trigonal axis is related to the volumes and shapes of the molecules comprising the HASPE lattice, and the volumes of any associated species such as counter ions.

The HASPE lattices can also be described in terms of the array of centroids of the SPEs: we use the symbol Ç for the centroid of an SPE, which in all cases except one is a centre of inversion in the lattice because the SPEs have exact $\bar{3}$ symmetry. The space group of the array of centroids is included in our tabulations of HASPE structures. The space groups encompassed by the HASPE lattices are both hexagonal and rhombohedral, and in Fig. 3 we remind the reader of the relationships between a primitive hexagonal lattice, a primitive rhombohedral lattice, and the description of a rhombohedral lattice with hexagonal axes as is common practice.

Occurrence of the HASPE Lattice

Our source of data is the graphical version of the Cambridge Structural Database (April 1997), which was screened first by selection of rhombohedral or hexagonal structures, then by occurrence of the phrase 'triphenyl' in the compound name. The lattice packing of each the 144 hits was then displayed and assessed visually for the occurrence of SPE interactions. We

recognise that this is not an exhaustive search protocol, and we have discovered other instances of HASPE lattices in general exploration of the structural database. Also, we describe below some *de facto* HASPE lattices which have lower crystallographic symmetry, and it is possible that there are many others. In the following, crystal structures are identified by their CSD reference codes, and the literature citations for these refcodes are listed at the end of the paper.

The molecular structures of the compounds revealed by this search include XR_3 moieties more elaborate than XPh_3, and can be grouped in four classes. The simplest molecular structure **A** is just XR_3; a larger class has a single atom or small group Y with three-fold symmetry attached to X (molecular structure **B**); a third class has a molecular structure **C** in which a linear spine connects XR_3 to another more distant possibly larger group with three-fold symmetry; the fourth class (**D**) has two XR_3 ends linked through a collection of atoms which also has three-fold symmetry.

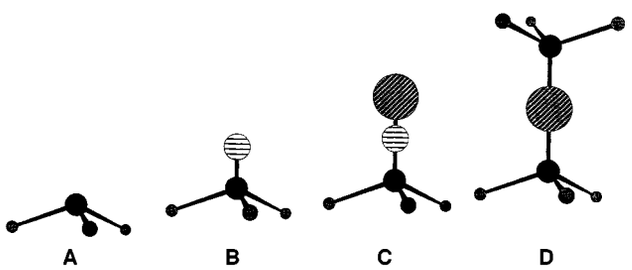

We describe the HASPE lattices by tabulating crystallographic details and presenting diagrammatic pictures of representative structures.

HASPE Lattices with Simple Molecules of Type A or B

Small simple molecules which crystallise with the HASPE lattice in space group $R\bar{3}$ are described in Table 1. There are four instances of a type **A** molecule, $As(C_6H_4OCH_3\text{-}4)_3$ and $E(C_6H_4CH_3\text{-}4)_3$ (E = P, As or Sb), which crystallise with virtually flat hexagonal nets, with good quadruple aryl embraces along all connections in the hexagonal net as well as the SPE between the nets. The 4-substituents do not interfere. The other four compounds in Table 1 have a different HASPE in space group $P\bar{3}$, which is illustrated in Fig. 4. There are two types of hexagonal net, one relatively flat and one puckered, with two flat nets and one puckered net in the cell repeat. There are two different SPEs, one between flatter nets and the other between puckered and flatter nets: the former SPE is shorter (C · · · C 5.91 Å in Ph_3CBr, TPHMBR02) and has crystallographic $\bar{3}$ symmetry, while the longer SPE at 6.24 Å has crystallographic symmetry 3 with a quasi inversion centre. The C · · · C distances within the flatter net are 8.13 Å, and in the puckered net are 8.44 Å. The Br atoms which are distal to each SPE are directed towards the centre of the contiguous hexagon [see Fig. 4(*b*)], and along the *c* axis point towards another Br atom, at a distance of 3.19 or 3.48 Å, within the sum of the van der Waals radii. As is partly evident from Fig. 4(*b*) there are QPE interactions along the 8.13 and 8.44 Å vectors of the hexagonal nets: the geometry of the longer interaction is actually a better QPE.

The compound Ph_3CCO_2H [ZZZVTS01] is noteworthy, because its carboxyl group cannot adhere to the three-fold symmetry of the molecular site, but this does not disrupt the HASPE which imposes rotational disordering of the carboxyl group about the three-fold axis: further, the normal hydrogen-bonded dimerisation of carboxyl groups occurs along the crystallographic *c* axis, through the centre of a hexagon.

HASPE Lattices with Molecules of Type B

A set of compounds with triphenylphosphonium cations (molecular structure type **B**) and various dianions also adopt the HASPE lattice. These compounds are described in Table 2. The HASPE lattice of $[Ph_3PH^+]_2\ [Ga_2Cl_6]^{2-}$ [FUPSEO] is portrayed in Fig. 5; the $[Ga_2Br_6]^{2-}$ and $[Ga_2I_6]^{2-}$ homologs are isostructural. There are short and tight SPEs which project alternately from either side of a virtually planar regular hexagonal network of P atoms. The anions, with a Ga–Ga bond and in staggered conformation, are positioned on three-fold axes at the centres of the hexagons, and therefore the H atoms of the phosphonium cations which are directed along three-fold axes are close to a triangle of Cl atoms at the end of an anion. Along each crystallographic three-fold axis the sequence is . . . $^+HPPh_3\cdot$ **SPE**$\cdot Ph_3PH^+ \cdot\cdot\ ^-[Cl_3GaGaCl_3]^- \cdot\cdot\ ^+HPPh_3\cdot$**SPE**$\cdot Ph_3PH^+ \cdot\cdot\ ^-[Cl_3GaGaCl_3]^-$. Along the edges of the hexagons (7.99 Å) there are well developed double phenyl embraces [see Fig. 5(*b*)]. The data in Table 2 show that as the size of the anion increases from $[Ga_2Cl_6]^{2-}$ to $[Ga_2I_6]^{2-}$ the length of the SPE is unchanged but the DPE expands to enlarge the hexagon.

Two compounds with Ph_3PCl^+ cations and $[MCl_6]^{2-}$ anions (M = Sn or Mo; see Table 2) demonstrate HASPE lattices very similar to that shown in Fig. 5. The SPE (P · · · P 5.6 Å) and DPE (P · · · P 7.6 Å) are short and tight. Note that in this crystal structure a Cl atom of the phosphonium cation is adjacent to a triangle of Cl atoms from the anion: this Cl · · · Cl distance is 3.8 Å in both compounds.

There are four compounds with Ph_3PMe^+ cations and dianions listed in Table 2, all in space group $R\bar{3}c$. One of these, with $[Cu_4I_6]^{2-}$, has virtually planar hexagonal nets like the HASPE structures just described, while the other three have strongly puckered hexagonal nets, elongated along the hexagonal axis. We have described and analysed the details of these crystal structures previously:[4] in the present context there are two important points to make. One is that the HASPE is elongated (in the $[CdBr_4]^{2-}$ and $[CdI_4]^{2-}$ compounds) or not (in the $[Cu_4I_6]^{2-}$ compound) in order to allow for the volume of the anion, which is prolate along the three-fold axis for the Cd anions and oblate for the Cu anion (all the anions being orientationally disordered). The second point is that the change in space group from $R\bar{3}$ to $R\bar{3}c$ is a consequence of the intimate relationship between the anions and the surrounding six cations in each hexagon, restricting rotational conformation of the Ph_3PMe^+ cations, and doubling the *c* repeat distance (see Table 2).

Also included in Table 2 are three compounds which form the HASPE lattice and contain two neutral species, JACWAL (JACWEP) contains Ph_3PO (Ph_3AsO) and toluene-*p*-sulfonamide in the ratio of 2:3. The SPEs formed here have P · · · P 6.47 Å but around the nearly planar hexagon there are only weak interactions consisting of single edge-to-face interactions. Distal to the SPE, where two O atoms of Ph_3PO are directed towards each other, each of three toluene-*p*-sulfonamide molecules bridges the two O atoms with hydrogen bonds from NH_2 (see below).

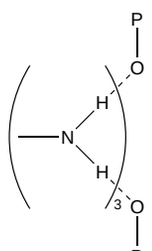

The complex with refcode BTZANI contains Ph_3PO and hexakis(benzotriazolyl)hexakis(vinylamine)trinickel(II). The SPEs are slightly longer than usual, at P · · · P 7.08 Å and the hexagonal net, which has P · · · P distances of 10.12 Å is slightly

Table 1 HASPE lattices formed by small simple molecules

Refcode[a]	Compound	Molecular structure class	Space group	Cell[b] axes *a*,*c*/Å	Crystallographic locations of X atoms[c]	Stacking of hexagonal nets[d]	SPE Length X···X/Å	Hexagonal X···X[e]/Å	Angle at X[d,f]/°	Aryl embraces in hexagonal net
BADBIR[g]	$As(C_6H_4OCH_3\text{-}4)_3$	**A**	$R\bar{3}$	13.3, 18.9	As, *c*	All layers identical	7.47	7.76	117.8 f	Good QPE
CANTEQ	$P(C_6H_4CH_3\text{-}4)_3$	**A**	$R\bar{3}$	12.6, 19.7	P, *c*	All layers identical	6.97	7.31	119.7 f	Good QPE
TOLARS01	$As(C_6H_4CH_3\text{-}4)_3$	**A**	$R\bar{3}$	12.7, 19.8	As, *c*	All layers identical	7.22	7.36	119.3 f	Good QPE
TPTOSB	$Sb(C_6H_4CH_3\text{-}4)_3$	**A**	$R\bar{3}$	12.8, 20.1	Sb, *c*	All layers identical	7.58	7.45	118.6 f	
JICWUN	$(C_6F_5)_3BPH_3$	**B**	$P\bar{3}$	15.1, 14.6	B, *c*,*d*,*d*	Repeat: f,p,f	6.19, 6.40	8.76	118.6 f	
								8.99	113.9 p	
TPHMBR02[h]	Ph_3CBr	**B**	$P\bar{3}$	13.9, 13.4	C, *c*,*d*,*d*	Repeat: f,p,f	5.91, 6.24	8.13	117.9 f	Poor QPE
								8.44	111.3 p	QPE
ZZZVTY12	Ph_3CCl	**B**	$P\bar{3}$	14.0, 13.2	C, *c*,*d*,*d*	Repeat: f,p,f	5.87, 6.30	8.18	117.6 f	
								8.52	110.5 p	
ZZZVTS01[i]	Ph_3CCO_2H	**B**	$P\bar{3}$	14.1, 13.1	C, *c*,*d*,*d*	Repeat: f,p,f	6.16, 6.24	8.28	116.9 f	
								8.54	111.3 p	

[a] Structure identifier used by the Cambridge Crystallographic Database. [b] Rhombohedral unit cells are described in the hexagonal axial setting. [c] Small italic letters identify the crystallographic special positions with three-fold local symmetry occupied by atoms X, according to ref. 6. [d] f = Flat hexagonal net; p = puckered hexagonal net. [e] X···X Distances within the hexagonal net. [f] X···X···X Angles within the hexagonal net. [g] Space group for Ç $R\bar{3}m$; OCH_3 occupies space between backs of SPEs. [h] Space group for Ç $P\bar{3}m1$. [i] CO_2H Group disordered, H bonding.

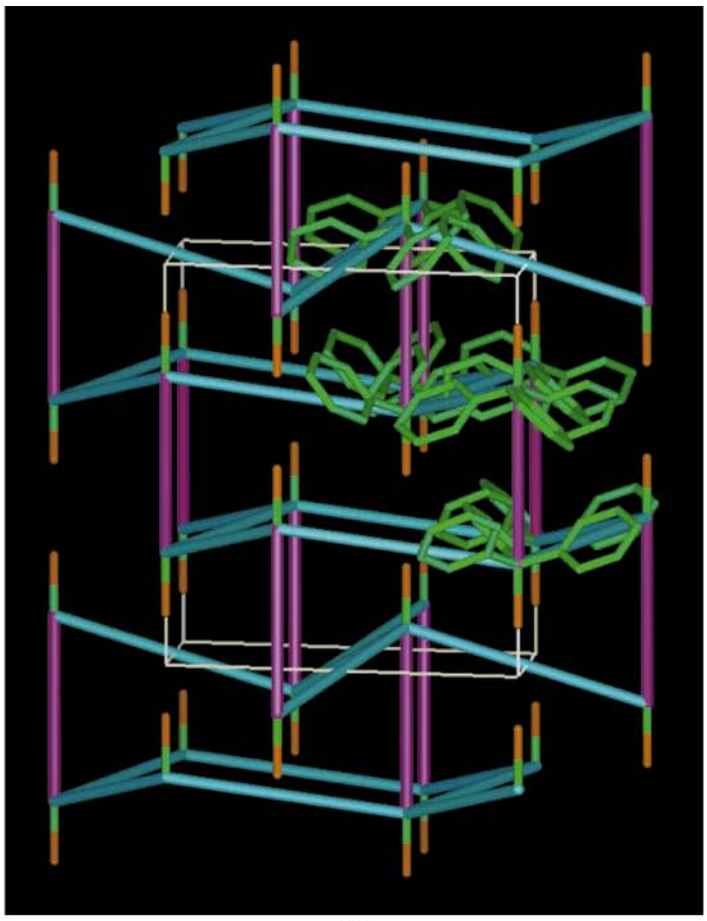

(*a*)

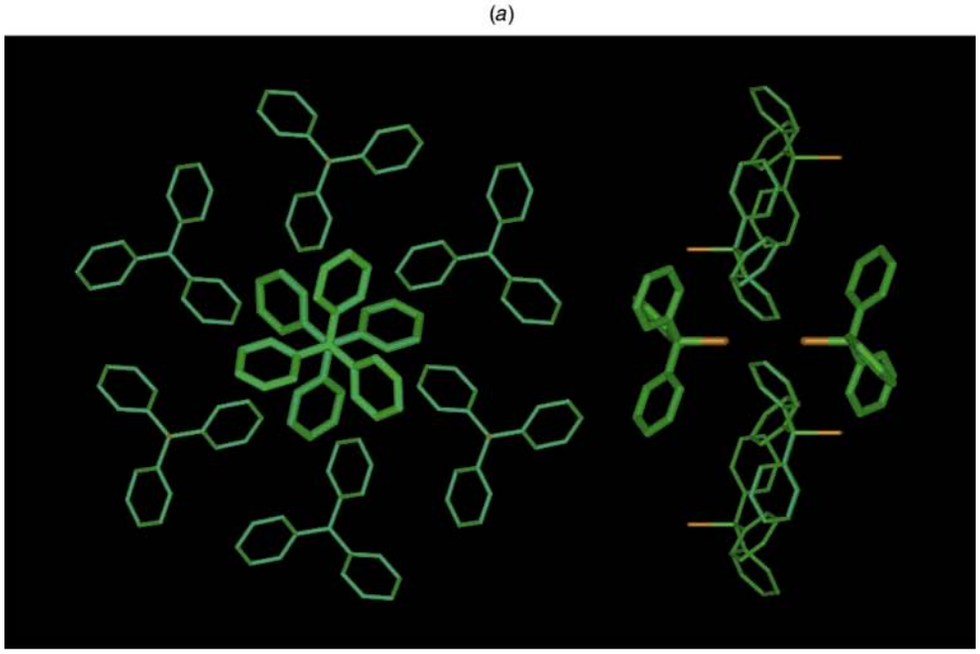

(*b*)

Fig. 4 Representations of the HASPE lattice in the crystal structure of Ph_3CBr [TPHMBR02], with the unit cell outlined (*c* vertical). (*a*) The net of supramolecular connections between the central C atoms, with all Br atoms included (orange). Each of the pink vertical rods is an SPE. The relatively flat and the puckered hexagonal nets are evident, as is the occurrence of two relatively flat nets and one puckered net in the repeat. Carbon atoms (green) for rings which form the two crystallographically independent SPE interactions are included. Note that all Br atoms (orange) point towards the centre of an adjacent hexagon. The blue rods signify the QPE interactions around the hexagons. (*b*) Top (*c* axis projection) and side views of Ph_3CBr molecules in a puckered hexagon (C green, Br orange) with the Br atoms of two adjacent molecules directed towards the centre of the hexagon: the Br · · · Br distance is 3.48 Å

puckered. The large size of the Ni cluster pushes the Ph_3PO molecules apart, so that there are no interactions around the hexagonal net. Instead, however, there are interactions between the Ph_3PO molecules and the aromatic rings of the Ni cluster. The phenyl ring of Ph_3PO which is directed towards the cluster takes part in one good **ef** interaction with one benzo

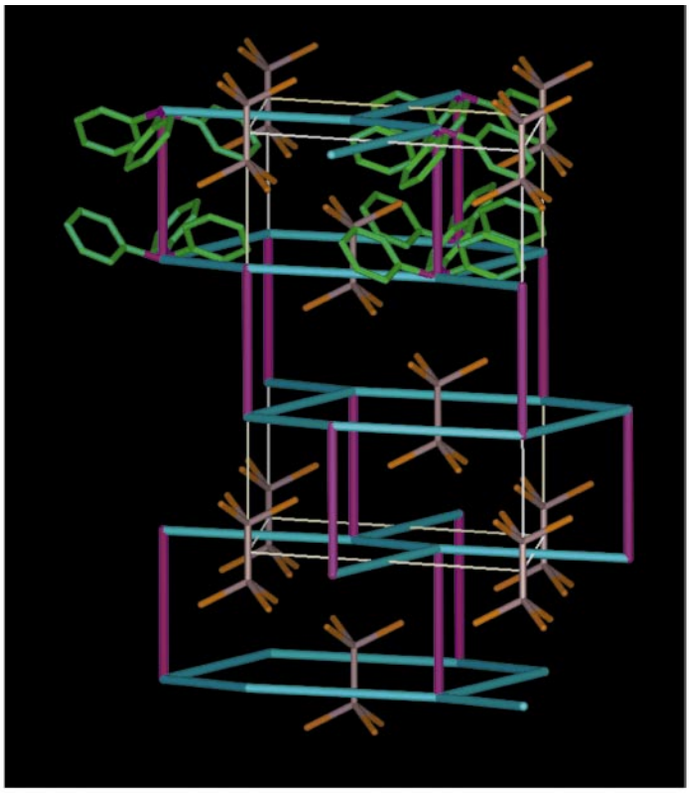

(*a*)

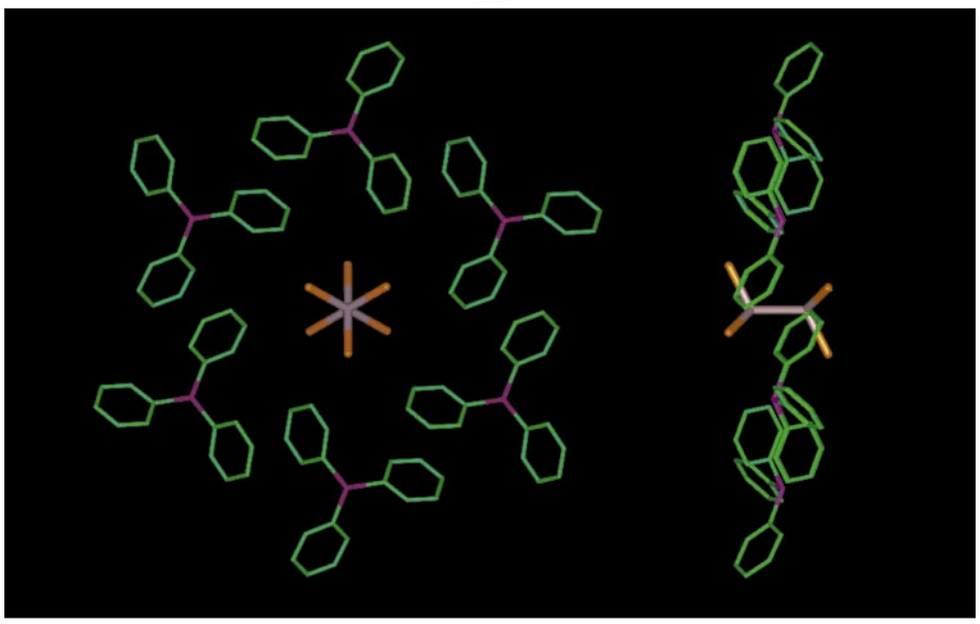

(*b*)

Fig. 5 (*a*) The HASPE lattice of $[Ph_3PH^+]_2\,[Ga_2Cl_6]^{2-}$ [FUPSEO]. The SPE are represented as pink rods, and the almost planar hexagonal nets by blue rods. The space group is $R\bar{3}$, with the hexagonal unit cell (with three times the contents of the primitive rhombohedral cell) outlined. Phenyl rings are marked for six cations in three SPE: the cation H atoms are omitted. All anions $[Ga_2Cl_6]^{2-}$ (with a Ga–Ga bond and Cl atoms in staggered conformation) are included (Ga fawn, Cl orange). (*b*) Three-fold and side views of one hexagon of Ph_3PH^+ cations centered by $[Ga_2Cl_6]^{2-}$. The DPE between adjacent cations are evident in the three-fold view: the distance between the centroids of the two phenyl rings of the DPE is 3.86 Å

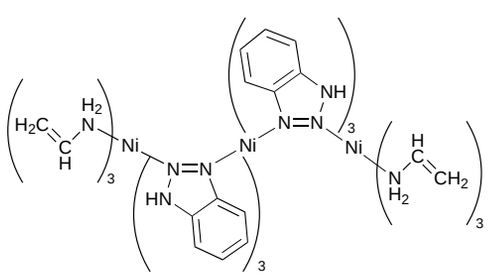

ring and a second somewhat distorted **off** interaction with another.

HASPE Lattices with Molecules of Type C

Table 3 provides details for HASPE lattices adopted by compounds in which XR_3 is at one end of a linear molecule, in some cases with a relatively large group at the other end. Fig. 6 shows the HASPE lattice in a representative structure in this class, namely $Ph_3POGaCl_3$. The space group is $R\bar{3}$ and the hexagonal net is almost planar. In this regard this structure is very similar

Table 2 HASPE lattices formed by triphenylphosphonium salts and triphenylphosphine oxide

Refcode[a]	Compound	Space group	Cell[b] axes *a*,*c*/Å	SPE length X···X/Å	Hexagonal X···X[c]/Å	Angle at X[d,e]/°	Aryl embraces in hexagonal net	Space group for X or Ç only
FUPSEO	$[Ph_3PH^+]_2[Ga_2Cl_6]^{2-}$	$R\bar{3}$	13.8, 17.6	6.23	7.99	119.8 f	Good DPE	X $R\bar{3}m$ Ç $R\bar{3}m$
FUPSIS	$[Ph_3PH^+]_2[Ga_2Br_6]^{2-}$	$R\bar{3}$	14.1, 17.6	6.20	8.13	119.9 f		
FUPSOY	$[Ph_3PH^+]_2[Ga_2I_6]^{2-}$	$R\bar{3}$	14.5, 18.3	6.24	8.39	120.0 f		
MPPICU	$[Ph_3PMe^+]_2[Cu_4I_6]^{2-}$	$R\bar{3}c$	14.0, 40.1	6.22	8.07	119.7 f	Good DPE	
MTPHCI	$[Ph_3PMe^+]_2[CdI_4]^{2-}$	$R\bar{3}c$	11.0, 64.0	6.74	7.45	94.9 p		X $R\bar{3}m$ Ç $R\bar{3}m$, $c' = c/2$
Ref. 4	$[Ph_3PMe^+]_2[CdBr_4]^{2-}$	$R\bar{3}c$	10.9, 59.2	6.39	7.18	98.4 p		
Ref. 4	$[Ph_3PMe^+]_2[CdBr_4]^{2-} + CH_2Cl_2$	$R\bar{3}c$	10.8, 62.4	6.78	7.22	97.1 p		
FUTPIT	$[Ph_3PCl^+]_2[MoCl_6]^{2-}$	$R\bar{3}$	13.2, 18.9	5.62	7.63	119.2 f	Good DPE	Ç $R\bar{3}m$
PINSOU	$[Ph_3PCl^+]_2[SnCl_6]^{2-}$	$R\bar{3}$	13.2, 18.9	5.59	7.63	119.2 f		
JACWAL[f]	$[Ph_3PO]_2[H_2NSO_2C_6H_4CH_3\text{-}4]_3$	$R\bar{3}$	18.7, 27.5	6.47	10.93	117.1 f	**ef** DPE	
JACWEP[f]	$[Ph_3AsO]_2[H_2NSO_2C_6H_4CH_3\text{-}4)_3$	$R\bar{3}$	18.8, 27.4					
BTZANI	$[Ph_3PO]$[Ni cluster][g]	$R\bar{3}c$	17.4, 50.5	7.08	10.12	118.3 sl p		

[a] Structure identifier used by the Cambridge Crystallographic Database. [b] Rhombohedral unit cells are described in the hexagonal axial setting. [c] X···X Distances within the hexagonal net. [d] X···X···X Angles within the hexagonal net. [e] f = Flat hexagonal net; p = puckered hexagonal net; sl = slightly. [f] These two structures are included in the data base with the incorrect space group *R*3, instead of $R\bar{3}$. There are no atomic coordinates for JACWEP but it is isomorphous and isostructural with JACWAL. [g] See text for structural formula of cluster.

Table 3 HASPE lattices formed by molecules of type **C**, with XR_3 at one end of a linear molecule

Refcode[a]	Compound	Space group	Cell[b] axes *a*,*c*/Å	SPE length X···X/Å	Hexagonal X···X[c]/Å	Angle at X[d,e]/°	Aryl embraces in hexagonal net	Space group for X or Ç only
FUFVAD	$(C_6F_5)_3Ge\text{–}GeEt_3$	$R\bar{3}$	12.2, 30.4	7.34	7.59	107.2 p	None	
KIFSOH	$Ph_3P\text{–}AlMe_3$	$R\bar{3}$[f]	14.3, 16.5	6.89	8.40	117.3 f	ODPE	
KIFSUN	$(2\text{-}CH_3C_6H_4)_3P\text{–}AlMe_3$	$R\bar{3}c$[f]	15.0, 34.2	6.48	8.68	119.2 f		
PIHGIW	$Ph_3As\text{–}GaI_3$	$R\bar{3}$	14.8, 16.6	6.62	8.64	118.4 f	ODPE	
JEJLEP	$Ph_3P{=}O\text{–}GaCl_3$	$R\bar{3}$	13.8, 18.4	6.42	7.95	119.9 f	DPE	
JEJLAL	$Ph_3P{=}O\text{–}AlCl_3$	$R\bar{3}$	13.7, 18.3	6.36	7.89	119.9 f	DPE	
JEJLIT	$Ph_3P{=}O\text{–}AlBr_3$	$R\bar{3}$	14.0, 18.4	6.36	8.10	119.9 f	DPE	
WAWKAG	$Ph_3P{=}O\text{–}AlMe_3$	$R\bar{3}$	13.8, 18.2	6.45	8.00	119.8 f	DPE	
WEKBIX	$Ph_3P{=}N{=}TiCl_3$	$R\bar{3}$	13.7, 18.5	6.38	7.92	119.9 f	Good DPE	
BAYFUC	$Ph_3P\text{–}Au\text{–}V(CO)_6$	$R\bar{3}$	13.6, 23.6	7.35	7.85	119.6 f	Good DPE	
CINSIB	$Ph_3P\text{–}Au\text{–}C(CN)Cl_2$	$R\bar{3}$	12.8, 21.1	6.91	7.38	120.0 f	Good DPE	
CIWZUD	$Ph_3Si\text{–}O\text{–}Si(CH{=}CH_2)_3$	$R\bar{3}$	14.8, 18.0	6.40	8.53	119.8 f	ODPE	
KOMMOO	$Ph_3Si\text{–}O\text{–}TiN(CH_2CH_2O)_3$	$R\bar{3}$	9.6, 45.4	6.91	9.57	120.0 f	Network of 1/2 interactions (see text)	X $R\bar{3}m$ Ç $R\bar{3}m$
WEWLEP	$Ph_3P\text{–}Au\text{–}Tc(NC_6H_3Pr^i_2\text{-}2,6)_3$	$R\bar{3}$	14.9, 39.6	6.49	10.93	86.2 p		X $R\bar{3}m$ Ç $R\bar{3}m$
FUTTAP	$Ph_3As\text{–}I\text{–}I + 1.5\ C_6H_5Me$[g]	$R\bar{3}c$	13.3, 53.9	6.59	8.05	111.5 p	Poor DPE	Ç $R\bar{3}m$ $c' = c/2$

[a] Structure identifier used by the Cambridge Crystallographic Database. [b] Rhombohedral unit cells are described in the hexagonal axial setting. [c] X···X Distances within the hexagonal net. [d] X···X···X Angles within the hexagonal net. [e] f = Flat hexagonal net; p = puckered hexagonal net. [f] Structures reported in both the publication and in the CSD in non-centrosymmetric space group, which gives half empty lattice. [g] Toluene disordered.

to that shown in Fig. 5, but the chemical difference is that the trihalogeno unit is part of the embracing molecule in the lattice rather than a separate entity as in Fig. 5, and the trihalogeno unit points towards the centre of a hexagon rather than away from it. Adjacent $GaCl_3$ ends of the molecule are directed towards each other, in staggered intermolecular conformation, as shown in Fig. 6(*b*). Other similar molecules have the same structure (Table 3), which occurs also with the $AlMe_3$ at the end of the molecule. The linearity at O in these molecules is unusual, and the original paper[7] alludes to possible disordering at this atom, in which case the HASPE lattice would be the overriding influence. There have been reports of cell dimensions for polymorphs of $Ph_3POGaCl_3$ in both orthorhombic and monoclinic space groups.[7]

Very similar HASPE lattices with almost planar hexagons occur for the chemically different compounds $Ph_3P\text{–}Au\text{–}V(CO)_6$ (in which the V co-ordination is octahedral distorted by the seventh Au ligand along the three-fold axis), and in $Ph_3As\text{–}GaI_3$ and $Ph_3Si\text{–}O\text{–}Si(CH{=}CH_2)_3$ where the DPE along the hexagon edge is longer and more offset. The compound $Ph_3P\text{–}Au\text{–}Tc(NC_6H_3Pr^i_2\text{-}2,6)_3$ has a much larger but three-fold entity at the end of the molecule, which requires that the hexagonal layers be severely puckered.

The compound $Ph_3Si\text{–}O\text{–}TiN(CH_2CH_2O)_3$ [KOMMOO] is terminated with a more compact three-fold entity, and adopts a HASPE lattice which is unique because all of the SPEs project from the same side of the hexagonal net (which is planar). This is illustrated in Fig. 7. All phenyl groups occur in the same plane (*i.e.* their centroids are coplanar) and within this plane there is a remarkable intermeshing of all phenyl groups, such that each phenyl ring in this plane has intermolecular interactions with four others around it. In this lattice there is complete segregation of phenyl–phenyl and alkyl–alkyl intermolecular interactions, and we regard this crystal lattice as being particularly informative about crystal supramolecularity.

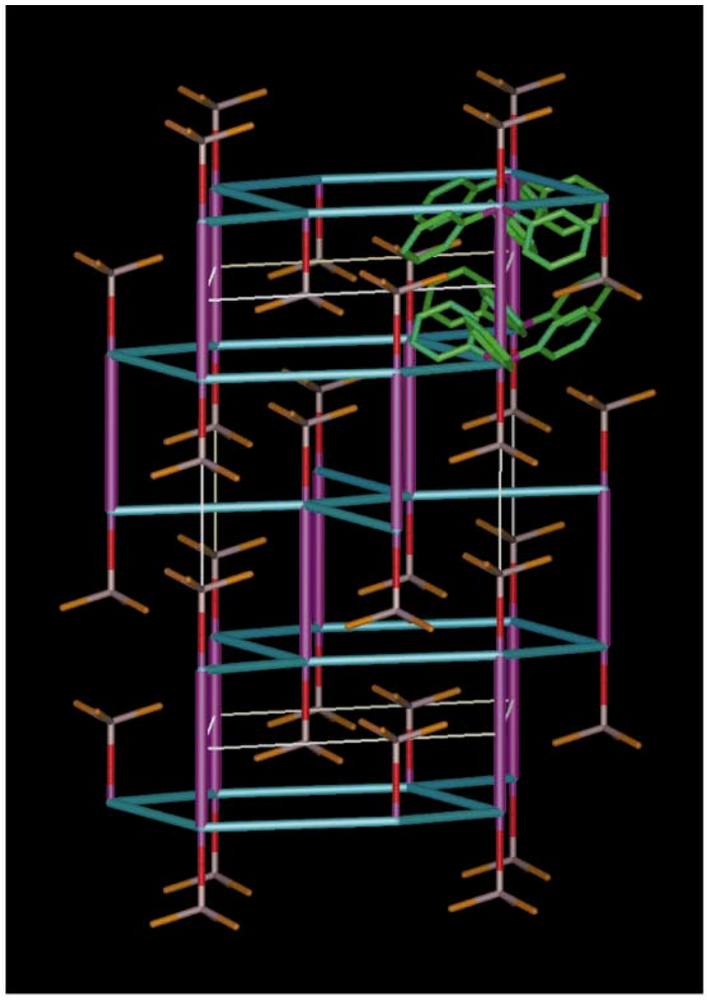

(*a*)

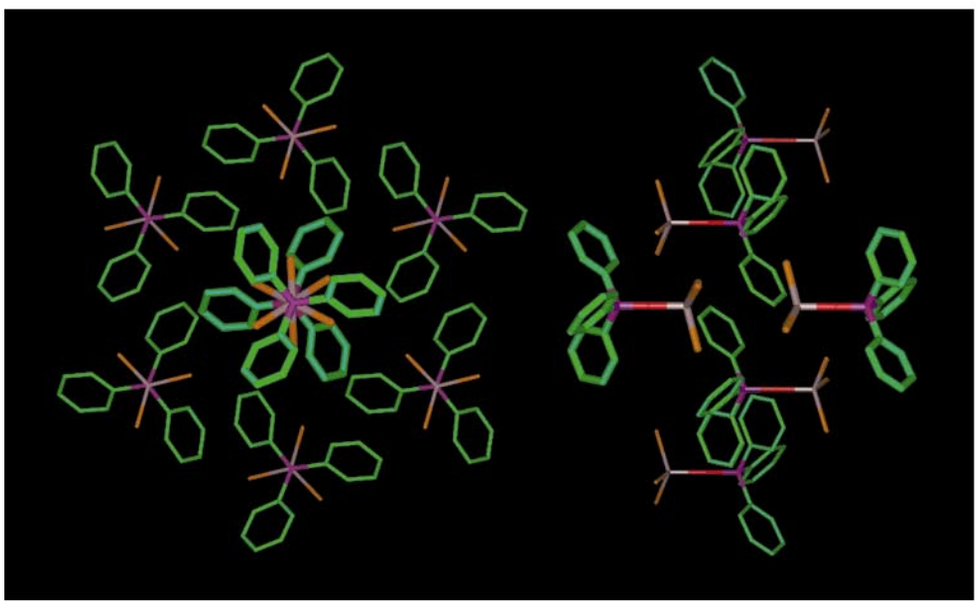

(*b*)

Fig. 6 The HASPE lattice structure of $Ph_3POGaCl_3$ [JEJLEP]. (*a*) The overall lattice, space group $R\bar{3}$, including details (green C atoms) of one SPE (pink rods) at a $\bar{3}$ site. O atoms are red, Ga fawn, Cl orange. (*b*) Three-fold and side views of the hexagon of molecules and two adjacent molecules with their $GaCl_3$ ends directed into the hexagon. The six DPE interactions around the edges of the hexagon are evident

HASPE Lattices with Molecules of Type D, with XR_3 at Both Ends

There is a class of molecules (Table 4) with three-fold symmetry and XR_3 groups at both ends. The lattice structures have similarities with those already described, but now the molecular sections distal to the XR_3 and the SPE are connected rather than simply pointing towards each other. Fig. 8 shows this structure for a relatively small molecule, $Ph_3P–Os(CO)_3–PPh_3$ [COSPHP], in which there is no symmetry operation relating

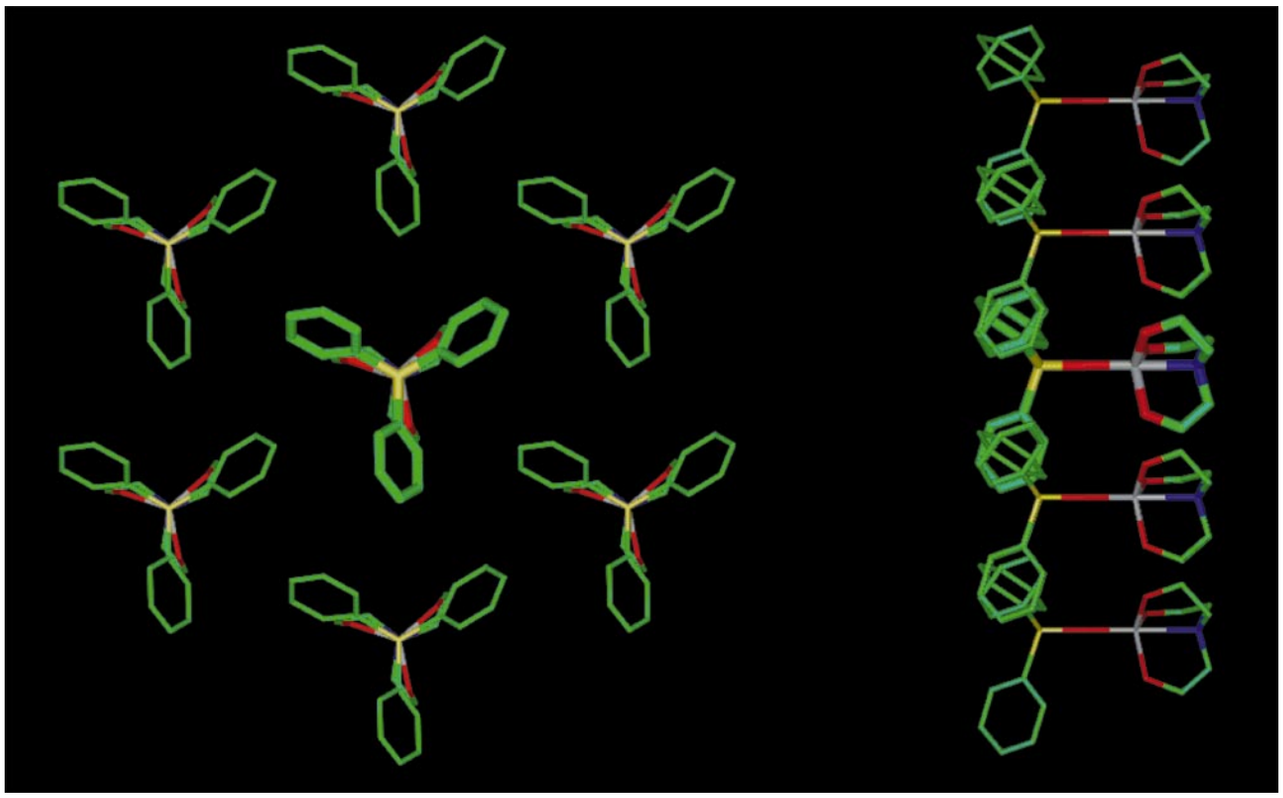

Fig. 7 Three-fold and side views of a centred hexagon on the HASPE lattice structure of $Ph_3Si–O–TiN(CH_2CH_2O)_3$ [KOMMOO]. Note that all of the Si atoms are in the same plane, and that the SPEs (not shown in full) project from the same side of this plane. Note also that all phenyl groups are in the one plane, within which each phenyl group has intermolecular attractive interactions with four other phenyl rings from three different molecules

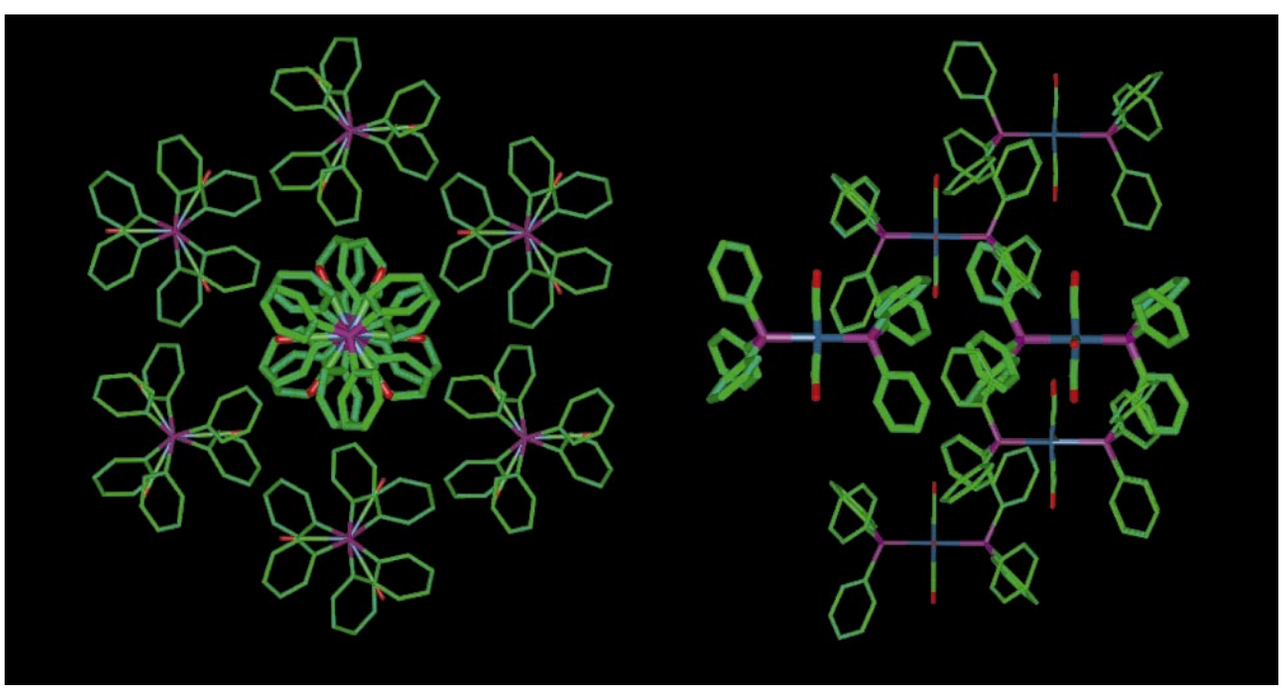

Fig. 8 Three-fold and side views of part of the crystal structure of $Ph_3P–Os(CO)_3–PPh_3$

the two ends of the molecule. Both ends, however, take part in SPE. The space group now has a *c* glide and an elongated *c* axis.

The larger complex $Ph_3P–Cu(\mu\text{-}SC_6H_4CH_3\text{-}4)_3–Mo–Cu(\mu\text{-}SC_6H_4CH_3\text{-}4)_3–PPh_3$ [SUDYUL] with octahedrally co-ordinated Mo at the centre forms a similar HASPE lattice. The 4-substituent leads to separation of molecules in the *ab* plane to leave triangular cavities which are occupied by disordered tetrahydrofuran (thf) molecules. This is shown in Fig. 9. The complex $Ph_3P–Cu(\mu\text{-}SPh)_3–U–Cu(\mu\text{-}SPh)_3–PPh_3$ [YIRHOW] is similar again, except that the molecules are pushed apart around the hexagonal net to accommodate disordered solvent in between. Aryl–aryl interactions around the hexagonal net are consequently precluded.

The complex $Ph_3Si–N=C=N–SiPh_3$ [TPSICI] is a significant molecule because the central stem is narrow (see Fig. 10). This crystal structure has many phenyl embraces in addition to the

Table 4 HASPE lattices formed by molecules of type **D**, with XR_3 at both ends of a linear molecule

Refcode[a]	Compound	Space group	Cell[b] axes *a*,*c*/Å	Crystallographic locations of X atoms[c]	SPE length X···X/Å	Hexagonal X···X[d]/Å	Angle at X[e,f]/°	Aryl embraces in hexagonal net	Space group for Ç only
COSPHP	$Ph_3P–Os(CO)_3–Ph_3P$	$P\bar{3}c1$	15.8, 23.2	P on *c*,*d*,*d* 3	6.83, 6.97	9.14	119.6 f	Ph · · Ph_2	Ç $P\bar{3}m1$ $c' = c/2$
DNTPIR	$Ph_3P–IrH(NO_3)_2–Ph_3P$	$P\bar{3}c1$	16.3, 22.8	P on *a*,*b*,*b* 3	6.74	9.47	119.1	Weak Ph · · Ph_2	
SUDYUL	$Ph_3P–Cu(\mu\text{-}SC_6H_4CH_3\text{-}4)_3–Mo–Cu(\mu\text{-}SC_6H_4CH_3\text{-}4)_3–PPh_3$ + 9thf	$R\bar{3}$	24.1, 16.6	P on 3	6.82	13.99	119.2	None	Ç $R\bar{3}m$
YIRHOW	$Ph_3P–Cu–(\mu\text{-}SPh)_3–U–(\mu\text{-}SPh)_3–Cu–PPh_3$ + 6thf	$P\bar{3}$	20.7, 17.6	P on *c*,*d*,*d* 3	7.03	11.99	119.4	None	
TPSICI	$Ph_3Si–N=C=N–SiPh_3$	$R\bar{3}$	15.0, 48.0	Si on 3,3,3,3	5.81, 6.74	8.78	118.0 sl p	PQPE	Ç $R\bar{3}m$
LIBHIN	$(4\text{-}CH_3C_6H_4)_3Pb–Ge(C_6H_4CH_3\text{-}4)_3$	$R\bar{3}$	13.3, 36.6	Pb/Ge[g] on 3	6.40	9.63	87.7 v p	*h*	
SOMMOW	$(4\text{-}CH_3C_6H_4)_3Sn–Sn(C_6H_4CH_3\text{-}4)_3$	$R\bar{3}$	13.3, 36.8	Sn on 3	6.37	9.67	86.9 v p	*h*	
SOMMUC	$(4\text{-}CH_3C_6H_4)_3Pb–Pb(C_6H_4CH_3\text{-}4)_3$	$R\bar{3}$	13.2, 37.4	Pb on 3	6.54	9.66	86.3 v p	*h*	
SOMNAJ	$(4\text{-}CH_3C_6H_4)_3Pb–Sn(C_6H_4CH_3\text{-}4)_3$	$R\bar{3}$	13.3, 37.2	Pb/Sn[g] on 3	6.50	9.69	86.6 v p	*h*	

[a] Structure identifier used by the Cambridge Crystallographic Database. [b] Rhombohedral unit cells are described in the hexagonal axial setting. [c] Small italic letters identify the crystallographic special positions with three-fold local symmetry occupied by atoms X, according to the International Tables for Crystallography. [d] X···X Distances within the hexagonal net. [e] X···X···X Angles within the hexagonal net. [f] f = flat hexagonal net; p = puckered hexagonal net; sl = slightly, v = very. [g] Metal atoms are disordered. [h] Embrace involving six rings. For each of a pair of molecules, one ring is from R_3X which is involved in the SPE and two are from the other XR_3.

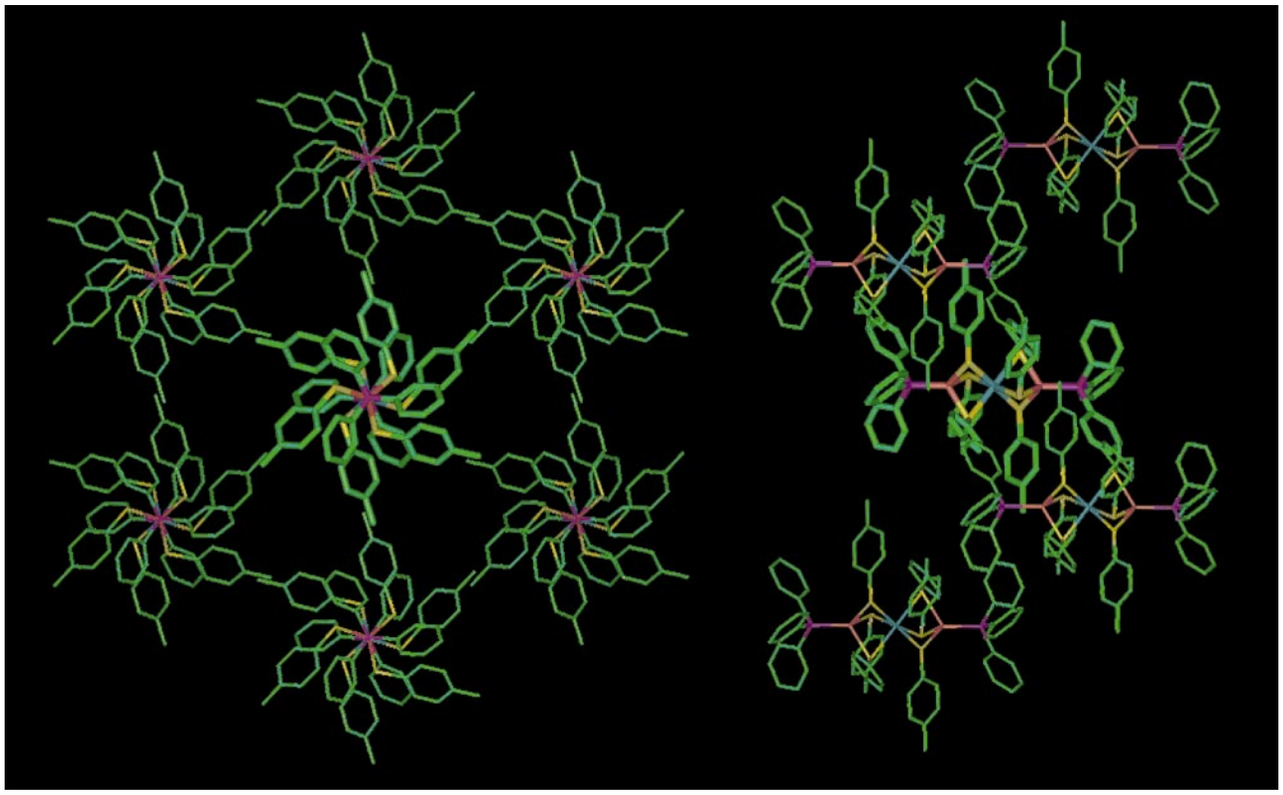

Fig. 9 The HASPE lattice in $Ph_3P–Cu(\mu\text{-}SC_6H_4Me\text{-}4)_3–Mo–Cu(\mu\text{-}SC_6H_4Me\text{-}4)_3–PPh_3$ [SUDYUL]. Disordered solvent molecules occupy the 'empty' spaces

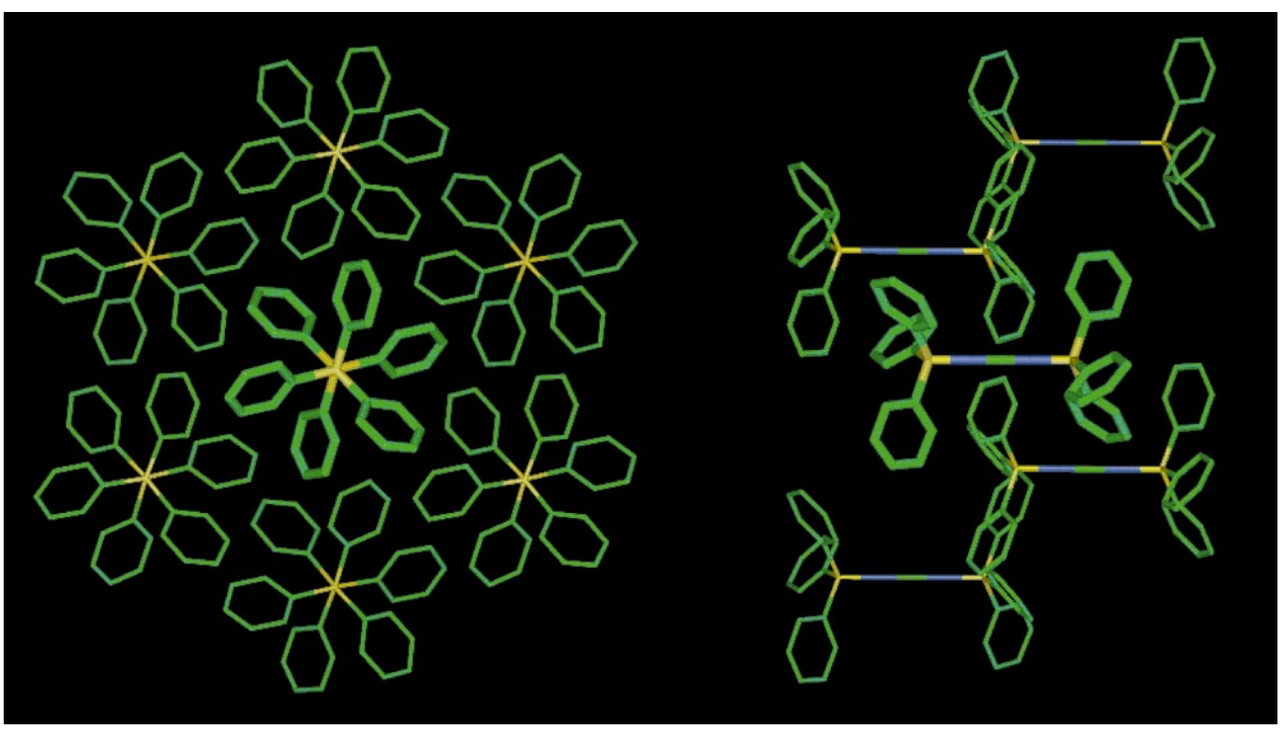

Fig. 10 Three-fold and side views of crystal structure of $Ph_3Si–N=C=N–SiPh_3$ [TPSICI]: N blue, Si yellow

SPE. Around the hexagonal ring, there are PQPE, while each ring of the molecule occupying the centre of the hexagon takes part in three **ef** interactions, two with one molecule of the hexagonal net, and one with a second. This is a classic wheel and axle compound, which as a consequence of the well-packed SPEs does not form an inclusion lattice.

All the type **D** molecules just described form HASPE lattices in which both ends of the molecule form SPEs. In contrast to this, there are four crystal structures listed in Table 4 which behave as though only one end of the molecule contained the XR_3 moiety. These are the four structures of the type $(4\text{-}MeC_6H_4)_3X–Y(C_6H_4Me\text{-}4)_3$, where X and Y are Ge/Pb [LIBHIN], Sn/Sn [SOMMOW], Pb/Pb [SOMMUC] and Pb/Sn [SOMNAJ]. In these structures, the molecules form only one SPE, and the HASPE lattice is similar to those described above for type **A**, **B** or **C** molecules. The space between non-interacting aromatic rings is occupied by the methyl groups protruding from surrounding molecules. For the mixed-metal

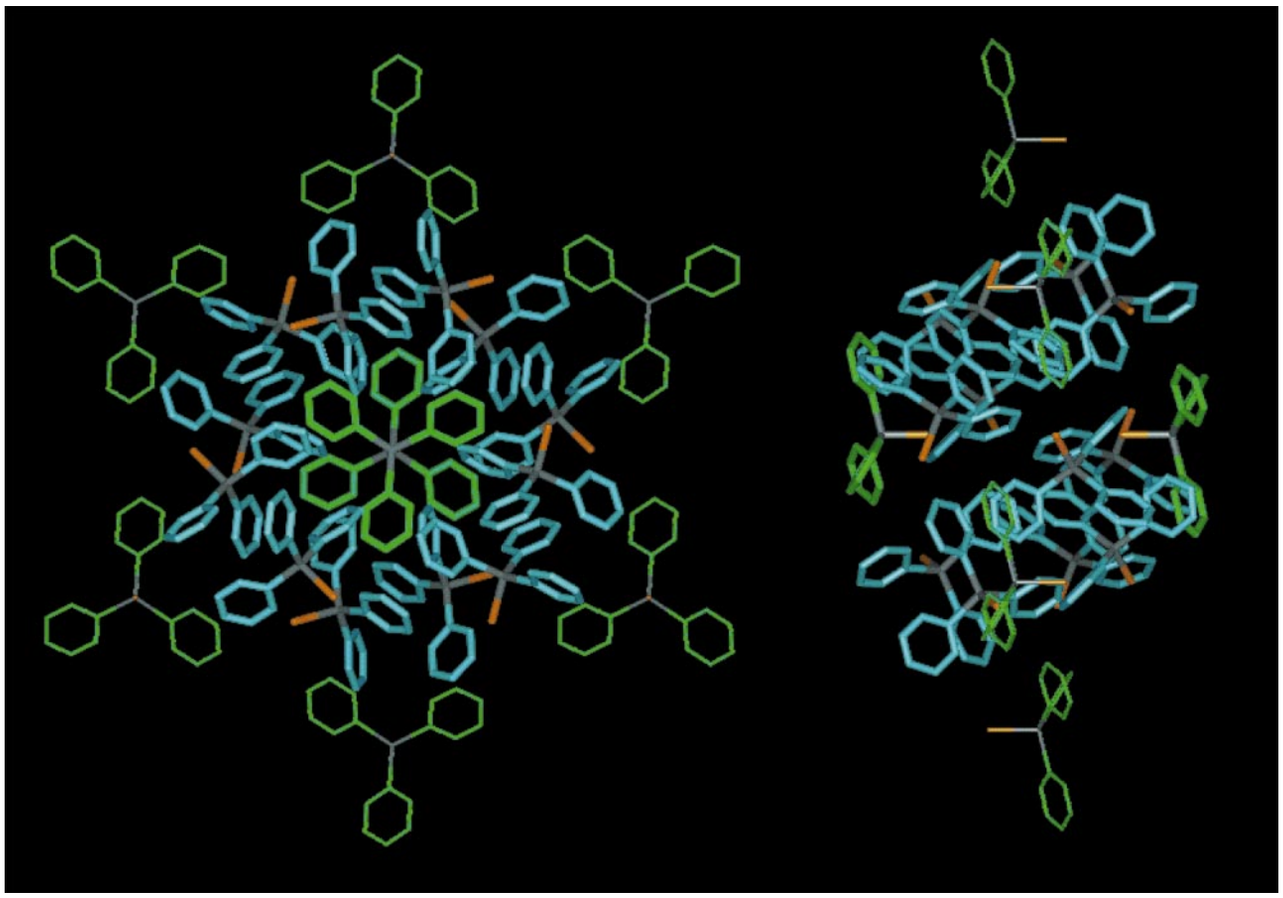

Fig. 11 Three-fold and side views of part of the crystal packing of the rhombohedral polymorph of Ph_3SnCl, illustrating the outer hexagonal net of molecules aligned with the three-fold axis (coloured green) and the inner hexagon of 12 molecules in six SPEs (coloured blue)

compounds, $(4\text{-}MeC_6H_4)_3Ge–Pb(C_6H_4Me\text{-}4)_3$ [LIBHIN] and $(4\text{-}MeC_6H_4)_3Sn–Pb(C_6H_4Me\text{-}4)_3$ [SOMNAJ], the metals are disordered over the two sites, so that for packing purposes, it is irrelevant which metal is at the 'end' of the molecule which forms the SPE.

The cation $[PN(PPh_3)_2]^+$ could be considered as suitable for the formation of this class of HASPE if the central PNP geometry is linear (which is often not the case). There are three hexagonal/rhombohedral crystal structure types including $[PN(PPh_3)_2]^+$ in the CSD, but none forms the HASPE lattice. In $[PN(PPh_3)_2]^+[M(CO)_6]^-$, M = Nb [BILNEP10] or Ta [BUVGII], the anion is situated *between* linear cations along the hexagonal axis. In the $[PN(PPh_3)_2]^+$ salt of the cluster $[(\mu\text{-}CO)_3(\mu_3\text{-}C{=}C{=}O)\{Ru(CO)_2\}_3(\mu_3\text{-}CuI)]^{2-}$[PAJWOM] there are two different columns in the *c* direction: in one, the anion is between cations, and in the second, there are only cations, but they are too far apart to embrace and are disordered. In $[PN(PPh_3)_2]^+[Fe_4(CO)_{13}]^-$[PIMNFE01] the cations are not linear and do not align with the hexagonal axis.

Unusual HASPE Lattices

The compound Ph_3SnCl [TPSNCL03] has a rhombohedral crystal lattice ‡ which has an additional unusual feature in which SPE interactions occur within the hexagons as well as between the hexagons. The hexagonal net of molecules with SPE occurring on opposite sides is similar to that in Ph_3CX (X = Cl or Br: see Fig. 4). However in the distal region of each of these SPE, where two Cl atoms point towards each other, there is another set of twelve Ph_3SnCl molecules not aligned with the crystallographic three-fold axis and which form a local hexagon of six SPEs. This is illustrated in Fig. 11. There are **ef** interactions between the two sets of molecules. Both types of SPE are remarkably short, 5.29 Å along the three-fold axis and 5.57 Å oblique to the three-fold axis.

The unconventional compound $[Ph_3As–I–I–I–AsPh_3]^+$ $[Ph_3AsCoI_3]^-$ [PELZAH], prepared in the solid state by reaction of Ph_3AsI_3 and $Co_2(CO)_8$, contains a mixture of double ended embracers and single ended embracers. The long *c* axis in space group $R3c$ is comprised of alternating $[Ph_3As–I–I–I–AsPh_3]^+$ and $[Ph_3AsCoI_3]^-$ species, which also alternate around the hexagonal lattice as shown in Fig. 12. The embrace sequence along the *c* axis is $\cdots Ph_3AsCoI_3\cdot\cdot Ph_3AsIIIAsPh_3\cdots Ph_3AsCoI_3\cdot\cdot$. The linearity of the central As–I–I–I–As segment is unusual, and is presumably a consequence of the HASPE lattice structure.

A chemically different and distinctive compound forming a HASPE lattice is $HOSi\{\eta^6\text{-}C_6H_5–Cr(CO)_3\}_3$, WAWXUN10, in space group $R\bar{3}$ (see Fig. 13). The SPE (Si···Si 6.45 Å) is formed by the $SiPh_3$ group, aligned with the three-fold axis, but the obverse face of each phenyl ring is η^6 bound to $Cr(CO)_3$. One of these CO ligands is directed almost parallel to the three-fold axis. Where the OH groups align along the three-fold axis, the O···O distance is 2.77 Å and there is presumably hydrogen bonding, although the hydrogen atoms are necessarily disordered.

Summary Account of the Symmetry and Dimensions of HASPE Lattices

All structures have SPEs aligned with the three-fold axis of the hexagonal or rhombohedral space groups. Analysis of the array of centroids Ç of the SPEs shows that all structures with only one X atom in the asymmetric unit have an array of centroids in

‡ There is also a monoclinic dimorph in which the interactions between the phenyl rings are not multiple embraces. The related compounds $ClSiPh_3$, $BrSnPh_3$ and $BrGePh_3$ have similar monoclinic lattices.

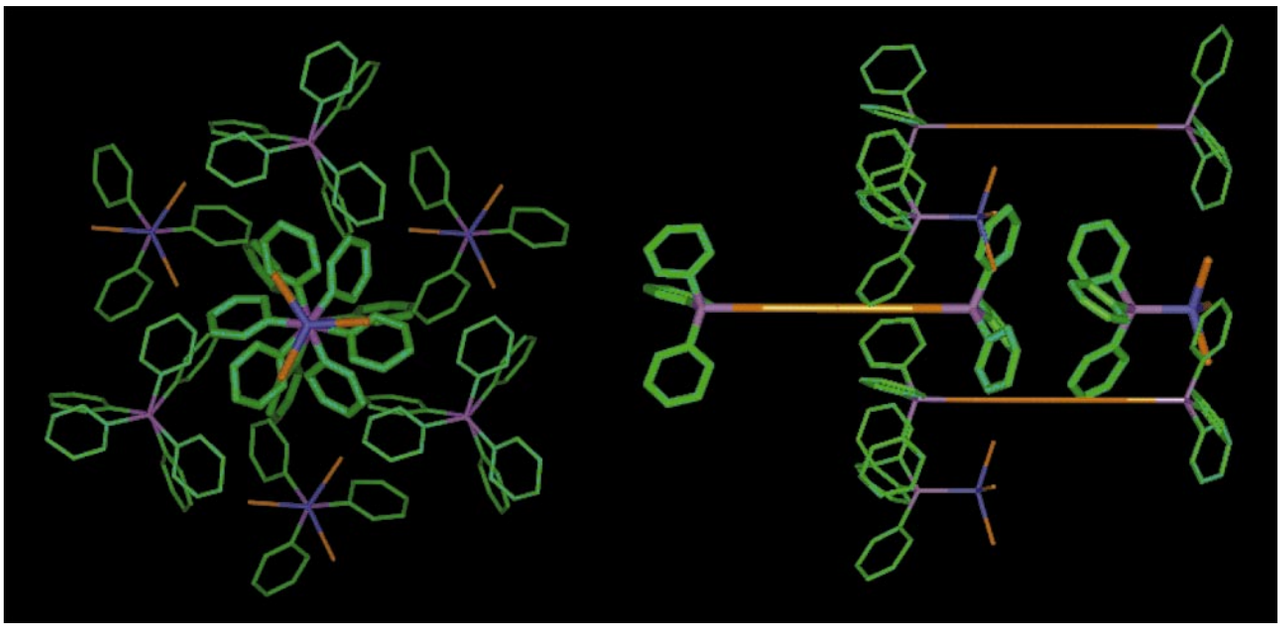

Fig. 12 Trigonal and side views of the HASPE lattice in crystalline $[Ph_3As{-}I{-}I{-}I{-}AsPh_3]^+[Ph_3AsCoI_3]^-$ [PELZAH]: Co blue, As fawn

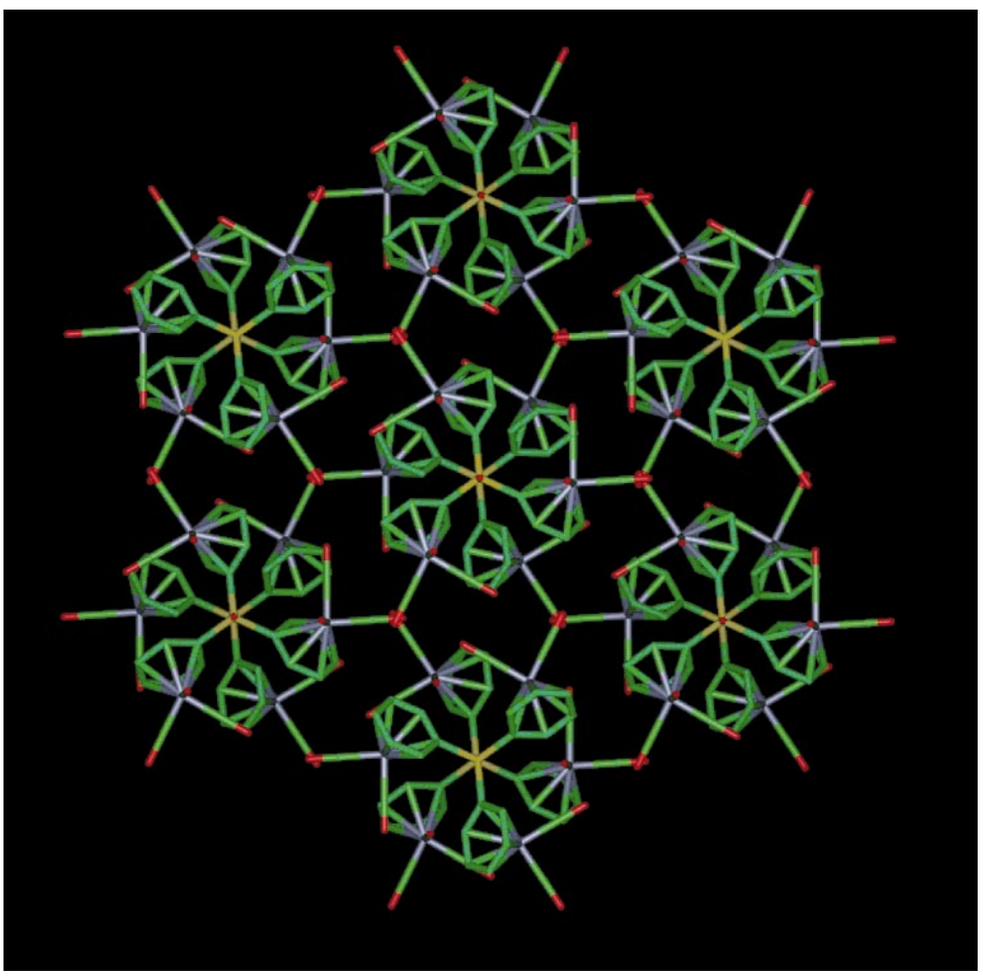

Fig. 13 Three-fold view of the crystal structure of $HOSi\{\eta^6\text{-}C_6H_5{-}Cr(CO)_3\}_3$, WAWXUN10: Si yellow, Cr white, space group $R\bar{3}$. Note that the O atoms of three CO groups from three different columns of SPE overlap along the three-fold axes between the columns of SPE

space group $R\bar{3}m$, irrespective of whether the space group of the complete structure was $R\bar{3}$ or $R\bar{3}c$, but for those in $R\bar{3}c$ the c repeat for the centroid array is half of c for the complete lattice. For those complete structures in space group $P\bar{3}$ or $P\bar{3}c1$, the asymmetric unit includes three different X atoms, and there are two independent SPEs (for example see Fig. 4): the arrays of SPE centroids can adhere to space groups $R\bar{3}m$ or $P\bar{3}m1$.

In all cases except one [KOMMOO], the SPEs around a hexagon of X atoms are directed alternately along $+c$ and $-c$. There is variety in the molecular sizes and shapes of YXR_3, with Y ranging from nothing [BADBIR] through single atoms, bulky three-fold units such as $Au{-}Tc(NC_6H_3Pr^i{}_2\text{-}2,6)_3$ [WEWLEP], short double ended connectors (N=C=N [TPSICI]), to bulky double ended connectors like Cu(μ-

Table 5

Refcode	X–Y · · · Y–X	*R*/Å	2 × SPE/Å	Angle at X/°	Ring geometry
FUPSEO	P–H · · · $Cl_3GaGaCl_3$ · · · H–P	11.3	12.5	119.8	Planar
PINSOU	P–Cl · · · $SnCl_6$ · · · Cl–P	13.3	11.2	119.2	Planar
FUFVAD	Ge–$GeEt_3$ · · · Et_3Ge–Ge	23.1	14.7	107.2	Elongated
WEWLEP	P–Au–Tc($NC_6H_3Pr^i_2$-2,6)$_3$ · · · ($NC_6H_3Pr^i_2$-2,6)$_3$Tc–Au–P	33.1	13.0	86.2	Elongated
BADBIR	As · · · As	11.4	14.9	117.8	Compressed
PIHGIW	As–GaI_3 · · · I_3Ga–As	9.9	13.2	118.4	Compressed

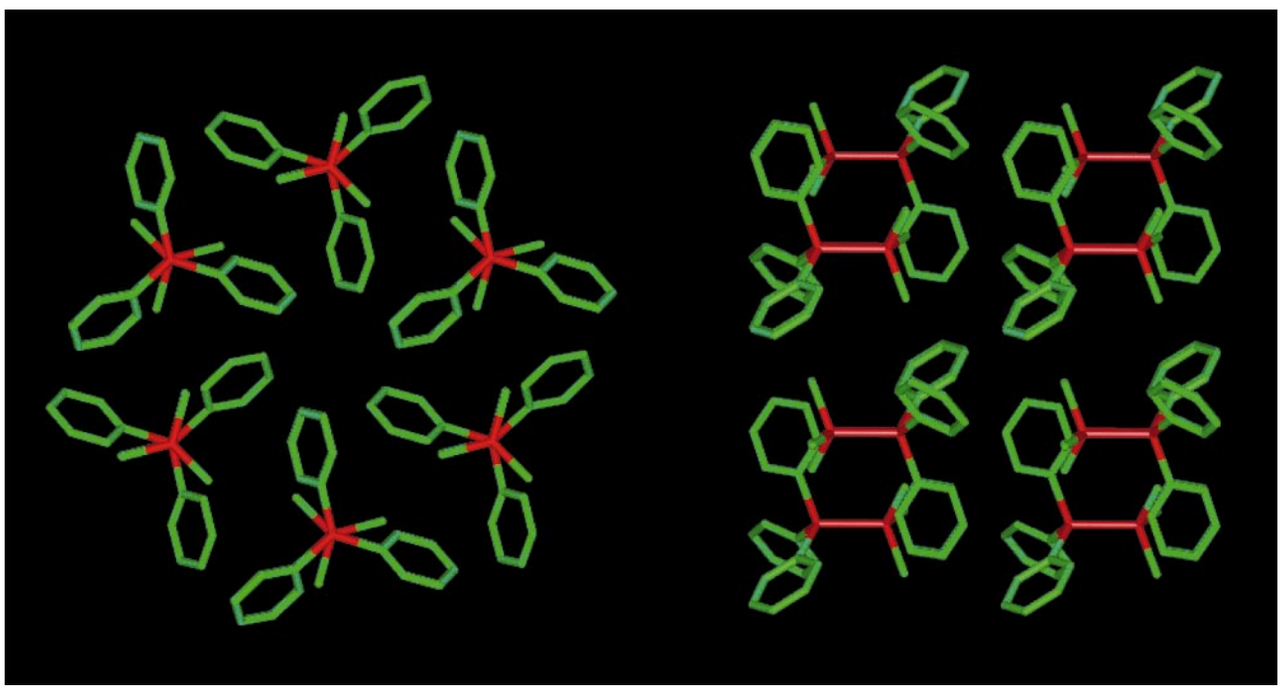

Fig. 14 The hexagonal lattice of Ph_3Ge–$GeMe_3$ [HAYSEF]: Ge red. The CH · · · Ph interactions are shorter around the hexagonal net than along the three-fold axis

$SC_6H_4CH_3$-4)$_3$–Mo–Cu(μ-$SC_6H_4CH_3$-4)$_3$ [SUDYUL]. This variety is accommodated by variation in the dimensions and puckering of the HASPE array of X atoms. The X · · · X lengths of the SPEs range from 5.59 to 7.58 Å (and 5.29 Å in the unusual lattice of TPSNCL03), but the X · · · X distances in the hexagons cover a much larger range, 7.18–13.99 Å. Where this $X \cdots X_{hexagon}$ distance is relatively short it signifies additional multiple phenyl embraces (QPE, DPE).

Compression or elongation of the lattice can be understood in the following way. Defining *R* as the length X–Y · · · Y–X, when $R = 2 \times SPE$, the hexagonal net is planar (Fig. 1). If *R* is greater than twice the SPE the hexagonal net must pucker by elongation [Fig. 2(*a*)], while when *R* is less than twice the SPE the hexagonal is compressed [Fig. 2(*b*)]. This is illustrated in Table 5.

HASPE Lattices without Trigonal Symmetry

Triphenylmethyl chloride, Ph_3CCl, is reported to crystallise with a number of polymorphs, although full details are not available. The compound with refcode ZZZVTY12, in space group $P\bar{3}$, has been described above. Two other polymorphs [ZZZVTY03, ZZZVTY04], both in space group $P\bar{1}$, do in fact contain columns of SPE in a pseudo HASPE lattice. In a recent report, the structure of Ph_3Si–C≡C–H with O=PPh_3,[8] which crystallises in space group $P\bar{1}$, has been shown to have four crystallographically different columns of molecules taking part in SPEs. The overall packing, however, is a pseudo HASPE array. It is more difficult to uncover low symmetry HASPE lattices from the CSD.

Exceptions

While two mixed triaryl, trialkyl derivatives Ph_3P–$AlMe_3$ [KIFSOH] and (2-$CH_3C_6H_4)_3P$–$AlMe_3$ [KIFSUN] form the HASPE lattice (Table 3), the related compounds Ph_3X–YMe_3, where X/Y = Si/Si [BIMSUL], Ge/Si [GAFGID], Ge/Ge [HAYSEF] or Si/Ge [SENYIT] do not. Instead, a hexagonal array is formed in which the triplet of methyl groups is directed towards the three phenyl rings of the adjacent molecule along the three-fold axis, as illustrated in Fig. 14. The difference between these two groups of related compounds is that the first set has molecules alternating in direction along three-fold axis, while the second set has all molecules stacked in the same orientation. These two structure types are informative about subtle differences of interaction energy between segregated aryl–aryl and alkyl–alkyl contacts, *versus* desegregated aryl–alkyl contacts. The shortest contacts between the methyl groups and phenyl rings, however, is around the hexagonal net, rather than along the three-fold direction. Also forming the latter type of hexagonal lattice is (*p*-$ClC_6H_4)_3AsO$ [DATDIL01] where the O atom interacts with the phenyl rings of the adjacent molecule, forming three C–H · · · O hydrogen bonds with C · · · O distances 3.22 Å and H · · · O 2.35 Å.

The structures SUDYUL and YIRHOW in Table 4 form the HASPE lattice despite the inclusion of solvent, thf. However, for structures such as Ph_3Ge–$GePh_3$ with benzene [HPGEBZ10], Ph_3Sn–$SnPh_3$ with benzene [VINXOF], Ph_3Si–O–$SiPh_3$ with benzene [CECXAJ01], and Ph_3Si–O–$SiPh_3$ with piperidine [DOHDOT], the solvent disrupts the SPEs and interacts itself with the three phenyl rings at one end of the molecule. The alternative interaction of benzene with Ph_3Sn–$SnPh_3$ in

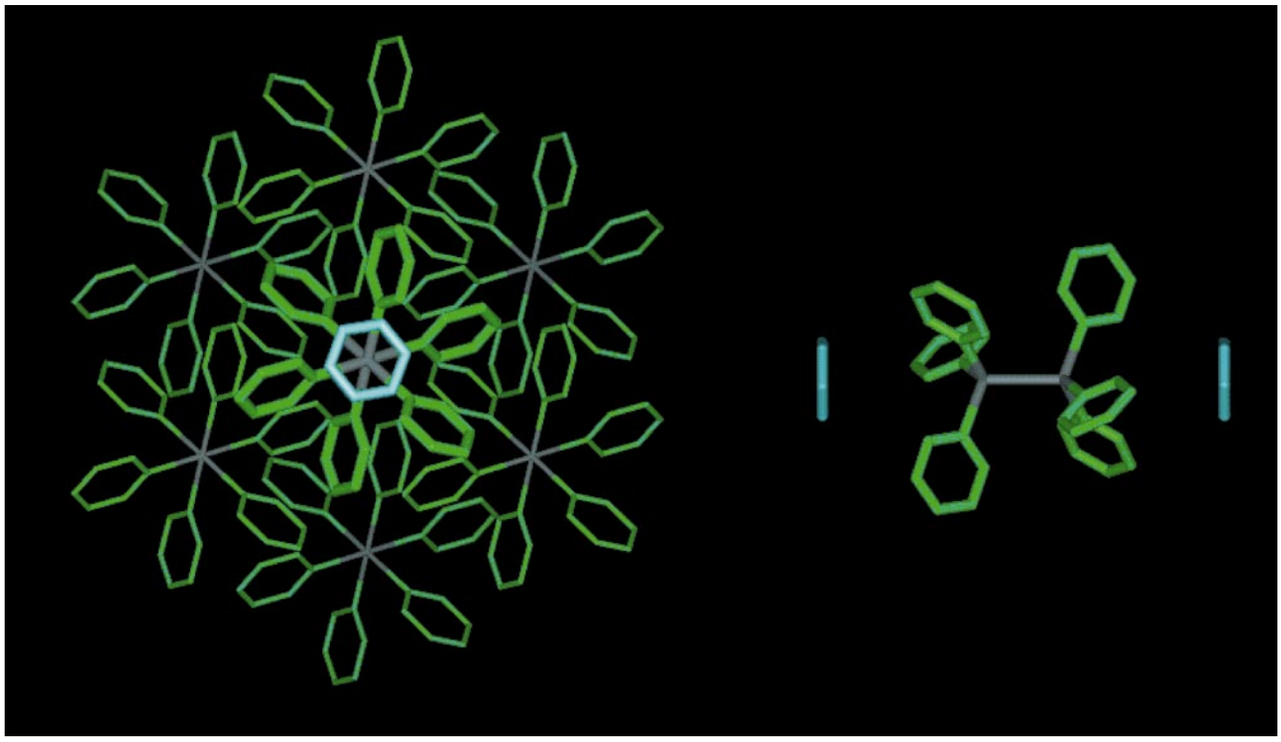

Fig. 15 Part of the structure of $Ph_3SnSnPh_3$ crystallised with benzene, showing how the benzene (blue) blocks the $SnPh_3$ face, obstructing the normal SPE formation

VINXOF is shown in Fig. 15. We believe that this alternative to the HASPE lattice occurs because the two XPh_3 ends of these short molecules have insufficient intramolecular separation to allow the intercolumn interactions of the HASPE lattice (see, for example, Fig. 10). In CECXAJ01 and DOHDOT ($Ph_3Si–O–SiPh_3$ with benzene and piperidine respectively) the geometry is linear at the O atom like the structures of $Ph_3P–O–GeCl_3$ [JEJLEP] and others in Table 3.

Conclusion

We have established (1) the generality of the HASPE lattice as a crystal supramolecular motif; (2) the variety of molecular structures which adopt this crystal supramolecularity; (3) the variability of the lattice to accommodate variations of molecular structure; (4) the dominance of the SPE and its contribution to lattice cohesion. The salts in which Ph_3PX^+ cations (X = Me, H or Cl) constitute the HASPE lattice are like inclusion structures with the anions located in cavities of the host lattice of sextuply embracing cations.

Acknowledgements

This research is supported by the Australian Research Council.

References

1 I. G. Dance and M. L. Scudder, *J. Chem. Soc.*, *Chem. Commun.*, 1995, 1039.
2 I. G. Dance and M. L. Scudder, *J. Chem. Soc.*, *Dalton Trans.*, 1996, 3755.
3 I. G. Dance and M. L. Scudder, *Chem. Eur. J.*, 1996, **2**, 481.
4 C. Hasselgren, P. A. W. Dean, M. L. Scudder, D. C. Craig and I. G. Dance, *J. Chem. Soc.*, *Dalton Trans.*, 1997, 2019.
5 F. H. Allen, J. E. Davies, J. J. Galloy, O. Johnson, O. Kennard, C. F. Macrae and D. G. Watson, *Chem. Inf. Comput. Sci.*, 1991, **31**, 204.
6 *International Tables for X-Ray Crystallography*, Kynoch Press, Birmingham, 1952.
7 N. Burford, B. W. Royan, R. E. v. H. Spence, T. S. Cameron, A. Linden and R. D. Rogers, *J. Chem. Soc.*, *Dalton Trans.*, 1990, 1521.
8 T. Steiner, J. van der Maas and B. Lutz, *J. Chem. Soc.*, *Perkin Trans. 2*, 1997, 1287.
BADBIR, TOLARS01, A. N. Sobolev and V. K. Belsky, *J. Organomet. Chem.*, 1981, **214**, 41.
BAYFUC, M. G. B. Drew, *Acta Crystallogr.*, *Sect. B*, 1982, **38**, 254.
BILNEP10, BUVGII, F. Calderazzo, U. Englert, G. Pampaloni, G. Pellizi and R. Zamboni, *Inorg. Chem.*, 1983, **22**, 1865.
BIMSUL, L. Parkanyi and E. Hengge, *J. Organomet. Chem.*, 1982, **235**, 273.
BTZANI, J. Meunier-Piret, P. Piret, J.-P. Putzeys and M. van Meerssche, *Acta Crystallogr.*, *Sect. B*, 1976, **32**, 714.
CANTEQ, A. N. Sobolev, V. K. Bel'skii, I. P. Romm and E. N. Gur'yanova, *Zh. Strukt. Khim.*, 1983, **24**, 123.
CECXAJ01, DOHDOT, K. Suwinska, G. J. Palenik and R. Gerdil, *Acta Crystallogr.*, *Sect. C*, 1986, **42**, 615.
CINSIB, E. G. Perevalova, Yu. T. Struchkov, V. P. Dyadchenko, E. I. Smyslova, Yu. L. Slovokhotov and K. I. Grandberg, *Izv. Akad. Nauk SSSR*, *Ser. Khim.*, 1983, 2818.
CIWZUD, A. I. Gusev, M. G. Los, S. D. Vlasenko, V. I. Zhun and V. D. Sheludyakov, *Zh. Strukt. Khim.*, 1984, **25**, 172.
COSPHP, J. K. Stalick and J. A. Ibers, *Inorg. Chem.*, 1969, **8**, 419.
DATDIL01, V. K. Bel'skii and V. E. Zavodnik, *J. Organomet. Chem.*, 1984, **265**, 159.
DNTPIR, D. N. Cash, R. O. Harris, S. C. Nyburg and F. H. Pickard, *J. Cryst. Mol. Struct.*, 1975, **5**, 377.
FUFVAD, R. I. Bochkova, Yu. N. Drozdov, E. A. Kuz'min, L. N. Bochkarev and M. N. Bochkarev, *Koord. Khim.*, 1987, **13**, 1126.
FUPSEO, FUPSIS, FUPSOY, M. A. Khan, D. G. Tuck, M. J. Taylor and D. A. Rogers, *J. Cryst. Spectrosc.*, 1986, **16**, 895.
FUTPIT, R. L. Richards, C. Shortman, D. C. Povey and G. W. Smith, *Acta Crystallogr.*, *Sect. C*, 1987, **43**, 2309.
FUTTAP, B. Beagley, C. B. Colburn, O. El-Sayrafi, G. A. Gott, D. G. Kelly, A. G. Mackie, C. A. McAuliffe, P. P. MacRory and R. G. Pritchard, *Acta Crystallogr.*, *Sect. C*, 1988, **44**, 38.
GAFGID, L. Parkanyi, C. Hernandez and K. H. Pannell, *J. Organomet. Chem.*, 1986, **301**, 145.
HAYSEF, L. Parkanyi, A. Kalman, S. Sharma, D. M. Nolen and K. H. Pannell, *Inorg. Chem.*, 1994, **33**, 180.
HPGEBZ10, M. Drager and L. Ross, *Z. Anorg. Allg. Chem.*, 1980, **469**, 115.
JACWAL, JACWEP, G. Ferguson and C. Glidewell, *J. Chem. Soc.*, *Perkin Trans. 2*, 1988, 2129.
JEJLAL, JEJLEP, JEJLIT, N. Burford, B. W. Royan, R. E. v. H. Spence, T. S. Cameron, A. Linden and R. D. Rogers, *J. Chem. Soc.*, *Dalton Trans.*, 1990, 1521.

JICWUN, D. C. Bradley, M. B. Hursthouse, M. Motevalli and Z. Dao-Hong, *J. Chem. Soc.*, *Chem. Commun.*, 1991, 7.
KIFSOH, KIFSUN, D. A. Wierda and A. R. Barron, *Polyhedron*, 1989, **8**, 831.
KOMMOO, W. M. P. B. Menge and J. G. Verkade, *Inorg. Chem.*, 1991, **30**, 4628.
LIBHIN, H.-J. Koglin, K. Behrends and M. Drager, *Organometallics*, 1994, **13**, 2733.
MPPICU, G. A. Bowmaker, G. R. Clark and D. K. P. Yuen, *J. Chem. Soc.*, *Dalton Trans.*, 1976, 2329.
MTPHCI, C. Couldwell and K. Prout, *Acta Crystallogr.*, *Sect. B*, 1978, **34**, 2312.
PAJWOM, A. S. Gunale, M. P. Jensen, D. A. Phillips, C. L. Stern and D. F. Shriver, *Inorg. Chem.*, 1992, **31**, 2622.
PELZAH, S. M. Godfrey, H. P. Lane, A. G. Mackie, C. A. McAuliffe and R. G. Pritchard, *J. Chem. Soc.*, *Chem. Commun.*, 1993, 1190.
PIHGIW, L.-J. Baker, C. E. F. Rickard and M. J. Taylor, *J. Organomet. Chem.*, 1994, **464**, C4.
PIMNFE01, G. van Buskirk, C. B. Knobler and H. D. Kaesz, *Organometallics*, 1985, **4**, 149.
PINSOU, E. Rentschler and K. Dehnicke, *Z. Kristallogr.*, 1994, **209**, 89.
SENYIT, K. H. Pannell, R. N. Kapoor, R. Raptis, L. Parkanyi and V. Fulop, *J. Organomet. Chem.*, 1990, **384**, 41.
SOMMOW, SOMMUC, SOMNAJ, C. Schneider and M. Drager, *J. Organomet. Chem.*, 1991, **415**, 349.
SUDYUL, P. M. Boorman, H.-B. Kraatz, M. Parvez and T. Ziegler, *J. Chem. Soc.*, *Dalton Trans.*, 1993, 433.
TPHMBR02, A. Dunand and R. Gerdil, *Acta Crystallogr.*, *Sect. B*, 1984, **40**, 59.
TPSICI, G. M. Sheldrick and R. Taylor, *J. Organomet. Chem.*, 1975, **101**, 19.
TPSNCL03, S. W. Ng, *Acta Crystallogr.*, *Sect. C*, 1995, **51**, 2292.
TPTOSB, A. N. Sobolev, I. P. Romm, V. K. Belskii and E. N. Gur'yanova, *J. Organomet. Chem.*, 1979, **179**, 153.
VINXOF, H. Piana, U. Kirchgassner and U. Schubert, *Chem. Ber.*, 1991, **124**, 743.
WAWKAG, F. J. Feher, T. A. Budzichowski and K. J. Weller, *Polyhedron*, 1993, **12**, 591.
WAWXUN10, K. L. Malisza, L. C. F. Chao, J. F. Britten, B. G. Sayer, G. Jaouen, S. Top, A. Decken and M. J. McGlinchey, *Organometallics*, 1993, **12**, 2462.
WEKBIX, T. Rubenstahl, D. W. von Gudenberg, F. Weller, K. Dehnicke and H. Goesmann, *Z. Naturforsch.*, *Teil B*, 1994, **49**, 15.
WEWLEP, A. K. Burrell, D. L. Clark, P. L. Gordon, A. P. Sattelberger and J. C. Bryan, *J. Am. Chem. Soc.*, 1994, **116**, 3813.
YIRHOW, P. C. Leverd, M. Lance, M. Nierlich, J. Vigner and M. Ephritikhine, *J. Chem. Soc.*, *Dalton Trans.*, 1994, 3563.
ZZZVTY12, A. Dunand and R. Gerdil, *Acta Crystallogr.*, *Sect. B*, 1982, **38**, 570.
ZZZVTS01, ZZZVTY03, ZZZVTY04, B. Kahr and R. L. Carter, *Mol. Cryst. Liq. Cryst. A*, 1992, **219**, 79.

Received 27*th August* 1997; *Paper* 7/06252D